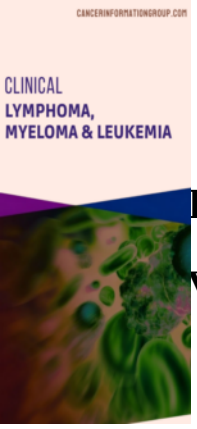

CLINICAL LYMPHOMA MYELOMA & LEUKEMIA
ISSN / eISSN 2152-2650 / 2152-2669
Publisher CIG MEDIA GROUP, LP,
3500 MAPLE AVENUE, STE 750,
DALLAS, USA, TX, 75219-3931
Volume 26-Issue 1-(2026)
DOI:https://doi.org/10.65281/702961

OPEN ACCESS

Long Non-coding RNA SNHG17 Exacerbates Spinal Cord Injury via the miR-381-3p/RAP1B Axis

Check for updates

Ming Jin [1], Wentao Wu [1], Zheyong Jia [1], Hu Qin [1], Yongxin Wang [1*]

1. Department of Neurosurgery,Xinjiang Medical University Affiliated First Hospital

Corresponding author: Yongxin Wang Email: xjdwy2000@sohu.com

Mailing Address: Department of Neurosurgery, Xinjiang Medical University Affiliated First H ospital Xinyiroad 373 street， Urumqi City, Xinjiang China.

Abstract

Objective: Severe traumas that affect The spinal cord and the central nervous system are known as spine injuries. LongNon-Coding RNAs (lncRNAs), which act as epigenetic adjusters, have the ability to affect neuronal apoptosis after SCI, the local inflammation environment, neuropathic pain, and vascular regeneration. Therefore, the research′s first purpose is to investigate the expression mode of lncRNA SNHG17 under the condition of SCI. Thus, it also intends to confirm SNHG17′s regulatory action in apoptosis and inflammation during SCI′s progression. Hence, The mechanism-based effects of SNHG17 will be verified through further in vivo and in vitro tests.

Methods: We first constructed a spinal cord injury cellular model by means of lipopolysaccharide-activated BV-2 microglial cells. We applied this method to measure the expression level of SNHG17. Additionally, A mouse brain injury model was developed to evaluate motor function using the Basso, Beattie, Bresnahan locomotor rating scale, footprint analysis, and grid-walking tests.Several functional tests were implemented in BV2 cells where SNHG17 or miR-381-3p had been modified, incorporating flow cytometry, west blot analysis, the use of the use of quantitative and the Cell Signalling Kit-8 assay. For spinal cord injury mice, adeno-associated virus was used to knock down SNHG17/RAP1B, Subsequently, histopathological evaluations were performed using haematoxylin and eosin staining, Terminal nucleotide transfers dUTP nick end labeling staining with Nissl exposure.Western blots and

qualitative DNA sequencing were used for molecular studies, and behavioral tests were performed. Hence, these assessments were conducted for the purpose of clarifying the in-vivo role of SNHG17.

Results: In spinal cord injury mice and BV2 cells treated with lipopolysaccharide, SNHG17 showed a very obvious upregulation. Therefore, under this situation, SNHG17 had the function to promote inflammation and apoptosis that are triggered by lipopolysaccharide. From the angle of mechanism, SNHG17 served as a competing endogenous RNA, which can sequester miR-381-3p. Thus, this action removed the inhibitory effect on RAP1B, which is the target gene of miR-381-3p. The SNHG17/miR-381-3p/RAP1B axis caused the worsening of microglial inflammation and neuronal impairment. Hence, when people carry out genetic removal of SNHG17, it can lead to the alleviation of motor deficits, the reduction of spinal cord inflammation, and the mitigation of tissue damage in spinal cord injury mice.

Conclusion: The long non-coding RNA (lncRNA) SNHG17 exacerbates the effects of neurological damage, which influences the miR-381-3p/RAP1B axis. Targeted inhibition of SNHG17 represents a potential therapeutic strategy to ameliorate SCI-associated motor dysfunction and neuroinflammation.

Keywords: Long non-coding RNA SNHG17; miR-381-3p/RAP1B axis; Spinal cord injury; Neuroinflammation; Apoptosis

Introduction

A brain injury is a dangerous illness that impairs the autonomic, voluntary, and nervous systems. Acute SCI is typically resulting from sudden outside force acting on the spine, which leads to vertebrae fracture and displacement [1, 2]. Up to 25 recorded secondary injury mechanisms have been identified following spinal cord injury (SCI), according to previous research.. Therefore, in recent period, researchers have developed various treatment methods that aim at the primary cellular and molecular pathophysiological changes in SCI. These changes include secondary injury mechanisms, the damage of broken spinal cord neuronal circuits, and the important functional losses caused by SCI [4, 5].a range of medications or techniques with neuroprotective characteristics are being developed to tackle secondary damage processes, such as factors related to inflammation and apoptosis [6, 7]. Furthermore,

other research has concentrated on modifying the signaling molecules that regulate neuronal development in order to promote the regeneration of severed spinal cord tracts [8, 9].

Non-coding ribonucleic acid (ncRNA) refers to RNA molecules which do not undertake protein-coding tasks. It mainly includes long non-coding ribonucleic acid (lncRNA), micro-ribonucleic acid (miRNA), as well as other unclassified RNA types. Recent study work has pointed out that spinal cord injury (SCI) can cause changes in lncRNA gene expression levels, and lncRNAs have an extremely important functional status in SCI. However, the mechanism through which lncRNA adjusts the expression of SCI-related genes remains not clear [10, 11]. A wide number of experimental investigations have convincingly revealed that there are considerable variations in lncRNA gene expression in situations involving spinal cord injury(SCI). The exact method by which long noncoding RNAs (lncRNAs) function in spinal cord damage is yet unknown. Therefore, gaining a more deep-level understanding about the function of lncRNA in SCI will be helpful for the establishment of SCI treatment methods.

A large number of research investigations have confirmed that microRNAs (miRNAs) occupy a very important status in the secondary injury processes of spinal cord injury (SCI). These processes include inflammation, angiogenesis, axonal regrowth, and glial cell development [13 - 17]. miRNAs control the expression of related proteins. They realize this goal by either raising or reducing the expression of target genes that have changes after SCI, therefore participating in the pathophysiological events of SCI . It must be stressed that the regulatory function of miRNA after SCI is complex and diversified. It involves multiple targets and signaling pathways, it is also impacted by several circumstances. Hence, future researches should make deeper exploration into the regulatory mechanisms of miRNA in SCI. This exploration will provide new concepts and methods for the treatment of SCI.

At present, the research about the influence of lncRNA upon spinal cord injury is in a limited state. The aim of this work aims to examine SNHG17 levels of expression in spinal cord injury (SCI) and its regulatory function in flare and apoptosis during SCI. Additionally, the study will use in vitro and in vivo tests to confirm SNHG17's legal operations. New molecular targets for clinical SCI treatment will be made available by further elucidation of the molecular mechanisms of SNHG74 in the development of spinal cord damage.

2 Materials and Methods

2.1 Experimental Animal Model

The female C57BL/6 mice utilized in this research weighed between 25 and 30 grams. The mice were supplied by the Animal Experiment Centre at Lanzhou University and housed in a clean-grade animal facility. The facility kept a climate of 21±2° C, a level of moisture of 40 ±10%. They also had at no cost utilization of nutrition and hydration. Every technique employed in the animal tests was approved by XXX (approval number XXX) and adhered to The protocols specified in the "Head of Laboratory Animal Care and Use Management." Before the experiment, the mice were given a week to get used to their surroundings before being divided into seven experimental groups at random: Shame, SCI, Sham + AAV - sgRNA - NC, SCI + AAV - sgRNA - NC, SCI + AAV - sgRNA - SNHG17, SCI + AAV - NC, and SCI + RAP1B overexpression (AAV - RAP1B). For the SCI group mice, the dosage was determined based on their weight before surgery, and they were anesthetized with 10mg/kg Xylazine (Yeasen Biotechnology (Shanghai) Co., Ltd., China) and 40mg/kg pentobarbital sodium. After fixation, shaving, and disinfection, the skin and subcutaneous tissue were incised to expose the spinal cord. A modified forceps was used to injure the tip of the spinal cord in a 4-5 mm area to a width of 0.1 mm, applying pressure for 2 seconds. The dura mater was kept intact and sutured afterward. A glass micropipette was used to inject sgRNA-NC, sgRNA-SNHG17, AAV-NC, and SCI + RAP1B overexpression adenovirus vectors into the epidural region on the dorsal and opposite sides of the spinal cord injury site in mice. All mice were euthanized under anesthesia on day 14 post-injury through intracardiac perfusion. After fixation, tissue samples were further immersed in 4% PFA for 2 hours, transferred to 0.2M phosphate-buffered saline (PB) at 4° C for 24 hours, Then, the tissues were cryoprotected in a 30% sucrose solution for 48 hours. Each team's mice's nerve root tissues were cut into segments surrounding the impact location that were 0.8 cm long, before being cut into 10 μm-thick, continuous transverse slices. Sections were collected every 100 μ m, with 10 sets of slices gathered for further analysis.

2.2 Animal Behavioral Experiments

Footprint analysis: To investigate how mice's hindlimb motor function recovers, a 10 cm wide and 150 cm long PVC square tunnel was constructed, with a dark chamber at the end and white paper lining the interior. Prior to the experiment, the mice's forelimbs were painted with red ink and their hindlimbs with blue ink, and they were placed at the beginning of the tunnel to be induced to move toward the dark chamber. After the mice walked through the tunnel, the paper with their foot marks was gathered and made dry, then changed into digital pictures for quantitative analysis. Stride length was taken as the index, therefore, longer stride length means the hindlimb movement ability of mice is better. Moreover, thus, three researchers used a double-blind way to carry out this test.

Foot Fault Test: First, mice carry out adaptive training on a specially made elevated horizontal ladder. In the experiment, when mice cross the ladder, paw slips, missteps and walking time are recorded by a video scoring system or sensors, and each mouse is tested four times. Walking skill level is measured by using a standardized foot fault scoring system for ladder walking 0–6 points. Therefore, the average finishing time, misstep number and other parameters are calculated. Thus, each category's score is multiplied by paw placement frequency and added together to get the overall score, which is the sum of forelimb and hindlimb scores. Hence, during testing, a stable and safe environment must be kept, and all staff members must receive professional training.

2.3 Basso Beattie Bresnahan (BBB) Scoring

The 21-point BBB scale was used to quantify the behavioral growth of mice with cerebral injuries; this scale ranges from 0, which means complete hindlimb inability to move, to 21, which stands for fully normal walking ability. Therefore, to conduct active tracking of the restoration progress, a comprehensive behavioral test was performed on the 13th day after surgery for the spinal cord injury mice. A double-blind experiment method was adopted; hence, three independent researchers were assigned the task to conduct detailed evaluation of the sensory and motor capabilities of the spinal cord injury mice, and this evaluation was implemented in a large space without any distracting factors. Therefore, to decrease the impact

of personal prejudices on the experiment results, three researchers' assessments were averaged to get each mouse's final behavioral score.

2.4 Experimental Cell Model

In this study, the BV-2 MCs cell line (mouse microglial cells) was purchased from Wuhan Pricella Biotechnology Co., Ltd. A complete culture medium was produced using 450 mL of RPMI-1640 basal medium (Hyclone, USA), 50 mL of 10% inactivated with heat fetal bull serum (Gibco, USA), and 5 mL of 1% penicillin-streptomycin solution (Hyclone, USA). A high-humidity incubator was used to maintain the cells at 37°C, with the atmosphere composed of 95% air and 5% CO2. Serum-free and antibiotic-free culture media was used in its stead prior to transfection. A transfection complex was created by combining the target plasmid (such as si-SNHG17) with Lipofectamine 2000 (Invitrogen, USA). This complex was then added to each well and left for 48 hours. Cells were transfected after 4 hours of LPS treatment, and the experimental groups were as follows: Control, LPS, Control + si-NC, LPS + si-NC, LPS + si-SNHG17, Control + empty vector, LPS + empty vector, LPS + SNHG17 overexpression, LPS + RAP1B overexpression, Control + NC mimic, LPS + NC mimic, LPS + miR-381-3p mimic, LPS + NC inhibitor + empty vector, LPS + miR-381-3p inhibitor + empty vector, LPS + miR-381-3p inhibitor + RAP1B overexpression, LPS + si-NC + NC inhibitor + empty vector, LPS + si-SNHG17 + NC inhibitor + empty vector, LPS + si-SNHG17 + miR-381-3p inhibitor + empty vector, LPS + si-SNHG17 + miR-381-3p inhibitor + RAP1B overexpression. The plasmids for SNHG17 (OE) and RAP1B were synthesized by BersinBio (Guangzhou, China), while the siRNAs targeting SNHG17 and RAP1B were synthesized by RiboBio. SNHG17's siRNA sequence is 5'-GGAGAGGATGCCTGGAAATAA-3’, with the corresponding control sequence (siNC) being 5’-AGGAGAACGAGTTAAGATGCG-3’. The siRNA sequence for RAP1B is 5’-TATGACCTAGTGCGGCAAATT-3’, and its control sequence (siNC) is 5’-GCGCTATCGAGATATGCTTAA-3’. Furthermore, GenePharma (Suzhou, China) created and produced the miR-381-3p mimic and inhibitor.

2.5 Quantitative RT-PCR

RNA was extracted using Trizol (Sigma-Aldrich, St. Louis, MO, USA). Subsequently, the entire RNA was reverse-transcribed into complementary DNA (cDNA). Reverse transcription

was performed using the Prime Script RT kit (Thermo Fisher Scientific, Waltham, MA, USA).Simultaneously, miR-381-3p was reverse-transcribed using the miRNA First-Strand Synthesis Kit (Takara, Tokyo, Japan). Subsequently, cDNA was utilized in qRT-PCR using the SYBR Green kit (Takara). GAPDH and RNU6 (U6) were used as natural standards to standardize the expression levels of lncRNA and miRNA. Respectively, The 2−△△Ct technique was used to determine the relative abundance. Sangon Biotech (Shanghai) Co., Ltd. produced the primers, which have the following sequences: TNF-α (5' -> 3')：Leading Primer-CTGAACTTCGGGGTGATCGG，Backward Primer-GGCTTGTCACTCGAATTTTGAG；IL-1β (5' -> 3')：Forward Primer-GAAATGCCACCTTTTGACAGTG，Reverse Primer-TGGATGCTCTCATCAGGACAG；IL-6 (5' -> 3')：Leading Primer-CTGCAAGAGACTTCCATCCAG，Reverse Primer-AGTGGTATAGACAGGTCTGTTGG；SNHG17：Leading Primer-GGGTCCAACAATACAGAGGA，Backward Primer-AAAACGTAACGTAATTCTGGCCAC；iNOS：Leading Primer-GTTCTCAGCCCAACAATACAAGA，Reverse Primer-GTGGACGGGTCGATGTCAC；RAP1B：Leading Primer-GCGGGTTAAAGACACTGATGA，Backward Primer--CTTGCTAGGTTCTGACCTTGTTC；Mmu-miR-381-3p：Leading Primer-CGCGTATACAAGGGCAAGCT，Backward Primer--AGTGCAGGGTCCGAGGTATT。

2.6 Flow Cytometry for Apoptosis Detection

Each group's cells were gathered, carefully resuspended in PBS, and then tallied. Five to ten times as many resuspended cells were collected, then the tissue had been spun at 1000 g for five minutes and the supernatant was collected.Annexin V-FITC binding solution (Shanghai Beyotime Biotechnology Co., Ltd.) was used to thoroughly clean the cells and adjust the concentration to 195 μl. The samples incubated for 10 to 20 minutes at ambient humidity in the shade before being evaluated right away using the Sony SA3800. Annexin V-FITC had green sparkle, while propidium iodide (PI) displayed red fluorescence.

2.7 Western Blot

RIPA lysis buffer (Keygen Biotech, Nanjing, China), SurePAGE gel (Thermo Fisher, Waltham, MA, USA), and the Midi-Cell electrophoresis system (XCell4 SureLock; Thermo Fisher) were used for target protein separation. A methanol-activated polyvinylidene fluoride (PVDF) membrane (Beyotime, Shanghai, China) was used for protein transfer. The membrane was incubated with the following primary antibodies: anti-Bcl2 (1:1,000, Cell Signaling Technology, USA), anti-Caspase3 and anti-Bax (1:1,000, Cell Signaling Technology, USA), a anti- β -actin and anti-RAP1B (1:1,000, Santa Cruz, USA), and anti-NeuN (ab181602, 1:10,000). It was then incubated with secondary antibodies (1:20,000, Abcam, (ab97051)) for 2 hours. The blot was visualized using ECL reagent (Beyotime). ImageJ was used to analyze the images, and The relative expression was determined using the formula.: Relative expression level = (Target value in experimental group / Intra-experimental value) / (Target value in control group / Intra-control value). The ECL reagent (Beyotime) was used to visualize the blot.

2.8 CCK-8 Assay

The CCK-8 detection method was used to carry out evaluation of cell proliferation ability. After cells had undergone 48 hours of transfection, 100 μL of the cultivation media with 10% fetal serum (FBS) was used to resuspend 1,000 cells. The cells were then put into a plate with 96 cavities. The plate was then incubated for two hours after 10 μL of Cell Counting Kit-8 (CCK-8) reagentwas applied to each well. A multi-well plate reader (BioTEK, USA) was then utilized to determine the absorbance of the solution at a wavelength of 450 nm.

2.9 Dual-Luciferase Reporter Gene Assay

In line with experimental regulations and group divisions, reporter-gene plasmids and other necessary plasmids were transfected into the cells; these plasmids were produced by Sangon Biotech (Shanghai) Co., Ltd. Each well was then filled with 100 μL of brand-new cell lysis buffer. In order to lyse the cells, the wells were then put through strong shaking on a vortex mixer or shaker during 15 minutes. After the cell lysis procedure finished, the The cell

lysate was gathered and then spun at 12,000 rpmrevolutions per minute for 20 minutes so as to remove impurities. A 10 μL sample of The liquid above the solid was collected and moved to a 96-well plate, and the Centro LB 960 microplate fluorescence detector was used to carry out quantification of the sample. After the detection work was completed, Renilla luciferase activity was utilized as an internal standard to make Firefly luciferase activity standardized. Hence, the relative luciferase activity corresponding to each well was finally calculated.

2.10 Hematoxylin-Eosin (HE) Staining and Nissl Staining

Tissues that have been embedded inside paraffin were cut into the wanted thickness. Therefore, the cut sections were first immersed in Xylene I and next in Xylene II, carrying out two cycles of xylene processing work.with deparaffinization performed for 10 minutes in each container.The slices were one by one put into a series of ethanol solutions with concentration gradient from high to low, with each soaking process lasting 2 minutes. Therefore, afterwards the slices were washed in distilled water. Hematoxylin and Eosin (HE) Staining: After deparaffinization, 4 μm sections were rehydrated using an ethanol gradient, followed by hematoxylin staining (2 min), differentiation in acidic ethanol (35 s), lithium carbonate immersion (55 s), 80% ethanol soaking (1 min), and eosin counterstaining. Nissl Staining Operation: 5-micrometer sections were treated with Nissl dye. Before staining activity, the dye was pre-heated to 60 degrees Celsius and kept at this temperature duration for 20 minutes. After staining process, sections were washed with distilled water. Therefore, differentiation and decoloration steps were implemented. This goal was achieved through utilization of 95% ethanol, until the section background showed clear distinction. Thus, after differentiation completion, sections experienced dehydration by ethanol application. After dehydration finish, xylene was used to perform section clearing. At last, sections were subjected to sealing measure. Stained section imaging was conducted by using a Leica DM4B microscope (Leica, Wetzlar, Germany). A Leica DFC550 camera (Leica, Wetzlar, Germany) was applied for taking section photographs under the microscope. For quantitative evaluation work, blinded assessment was carried out. Three sections were randomly chosen from each organ, hence for each selected section, at least three representative high-power fields (HPF, magnification of × 40) were inspected and analyzed.

2.11 TUNEL Staining

At first, cell or tissue samples were immersed into an ion-reduced buffer liquid. After this operation, they were fixed under surrounding temperature for a time period of 10 to 15 minutes. 4% paraformaldehyde or other fixing materials were used in this fixation procedure, and this procedure was followed by several times of washing steps. Next, the fixed samples were put into a solution which contains 0.5% Triton X-100 or other water-loving chemical substances to reach permeabilization purpose. After this step finished, the samples were washed one more time. Subsequently, a sufficient quantity of TUNEL reaction solution, produced by Yeasen Biotechnology (Shanghai) Co., Ltd., China. Subsequently, The samples were kept at 37° C for a duration of 1 to 2 hours. After the incubation process, add the preheated washing and reaction termination buffers. Place the samples in an incubator at 37 ° C for 30 minutes, then perform several washing steps. apoptotic cells identified a fluorescence microscope. The microscope was configured with an emission filter of 515 – 565 nm and an excitation wavelength of 450 – 500 nm.

2.12 Statistical Analysis

SPSS 17.0 software was used to statistically evaluate the data that was gathered. The mean ± standard deviation is used to display quantitative data. To evaluate the distinctions between these two groups, the t-test was employed. Use one-way ANOVA for comparing several data sets. A p-value below 0.05 was regarded as statistically significant.

3 Results

3.1 High Expression of SNHG17 in SCI Mice and LPS-Induced BV2 Cells

Mouse SCI microarray data were retrieved from the GEO database, obtaining sequencing datasets GSE132242 (including lncRNA and mRNA) and GSE158194 (miRNA). After we

carry out screening of platform data marked as GPL26743 - 199362 and review of related literature, deep analysis of mouse spinal cord injury (SCI) microarrays obtained from GEO database shows that long non-coding RNA SNHG17 was largely increased in SCI cases. Therefore, SNHG17 may have important function in SCI-related biological mechanisms. Hence, we select SNHG17 as research focus as shown in Figure 1A. After that, we successfully build a mouse model of SCI. Fourteen days after SCI induction, we perform Basso, Beattie, and Bresnahan (BBB) scoring on each experimental group. Scoring results display that, compared with control (sham) group, SCI group has obviously damaged hindlimb motor function; this is proved by a much lower BBB score refer to Figure 1B. Furthermore, Figure 1C demonstrated that the expression levels of tumor necrosis factor-α, interleukin-1β, and interleukin in the spinal cord tissue of spinal cord injury mice were significantly higher compared to the sham-operated group. As shown in Figure 1C, analysis results show that the spinal cord tissue of SCI mice has higher expression levels of tumor necrosis factor-alpha (TNF-α), interleukin-1 beta (IL-1β), and interleukin-6 (IL-6) than the sham group.The outcomes of these research works prove we have successfully built the spinal cord injury (SCI) mouse model. The expression of host gene 17 in small nucleolar RNA in spinal cord was detected by reverse transcription quantitative polymerase chain reaction: it is demonstrated that the expression of SNHG17 in the spinal cord injury (SCI) group is elevated compared to that in the sham group (Figure 1D). To copy the occurrence process of SCI in a test-tube environment, we established a neuroinflammation model; this work was finished by using lipopolysaccharide (LPS) to stimulate BV-2 microglial cells (MCs). Thus, RT-qPCR results show that the lipopolysaccharide-treated group (LPS group) has higher levels of inducible nitric oxide synthase (iNOS), tumor necrosis factor-alpha (TNF-α), interleukin-1 beta (IL-1β), and interleukin-6 (IL-6) than the normal control group (Control group) (Figure 1E). According to flow cytometry detection results, Figure 1F shows that the lipopolysaccharide (LPS) group had a larger percentage of apoptotic cells than the control group. Therefore, these results indicate that we have successfully established an in-vitro spinal cord injury (SCI) cell model. Therefore, reverse transcriptase quantitative polymerase chain reaction (RT-qPCR) was used to measure the amount of small nucleolar RNA host gene 7 (SNHG7) in cells from each group. The results demonstrated that SNHG7 expression levels in LPS-treated BV-2 cells had clearly increased in comparison to control group cells (Figure 1G). Hence, the above-mentioned results suggest that SNHG7 may have a regulatory action in LPS-induced BV-2 cells.

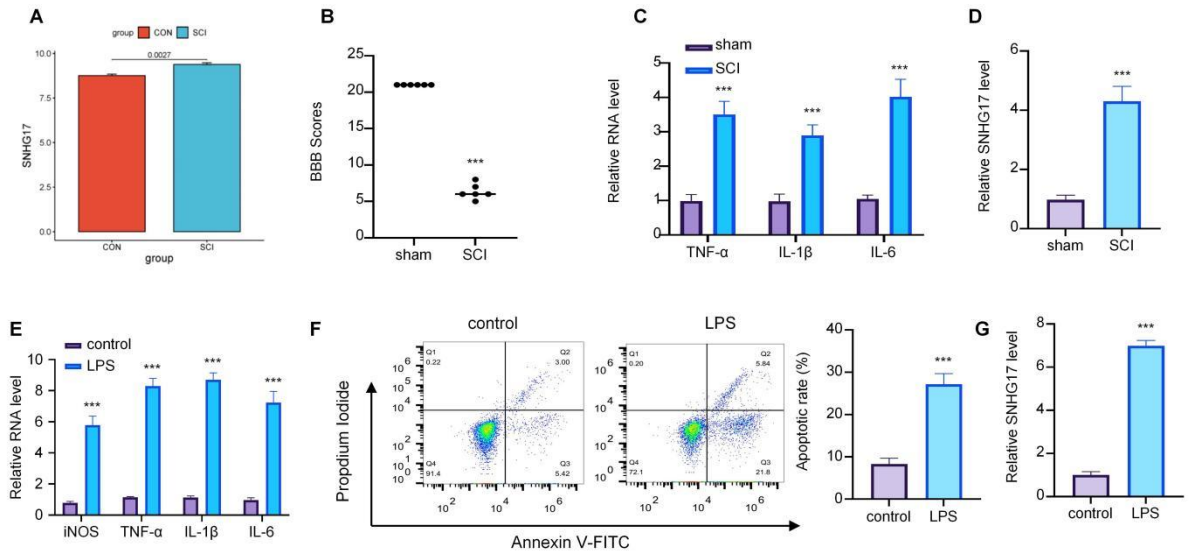

Figure 1. High expression of SNHG17 in SCI mice and LPS-induced BV2 cells.

3.2 SNHG17 Promotes the Inflammatory Response and Apoptosis in LPS-Induced BV2 Cells

For the purpose of probing into the special functions of SNHG17, we changed its expression level in BV2 cells through utilization of small interfering RNA or overexpression plasmids. The expression levels of inducible nitric oxide synthase, tumor necrosis factor-α, interleukin-1 beta, and interleukin-6 across different cell groups were then measured using reverse transcription quantitative polymerase chain reaction (qPCR). It was demonstrated that when SNHG17 was silenced, levels of iNOS, TNF-α, IL-1β, and IL-6 decreased;therefore, overexpressing SNHG17 brought about an increase of these cytokines. Cell apoptosis levels were higher when SNHG17 was overexpressed, according to flow cytometry data, which showed that cell apoptosis was decreased in the SNHG17 knockdown group. The SNHG17 knockdown group had higher cell viability, according to the Cell Counting Kit-8 assay. In contrast, the SNHG17 overexpression group showed decreased cell viability.Hence, all above results suggest that SNHG17 promotes the inflammatory response and apoptosis in lipopolysaccharide-induced BV2 cells.

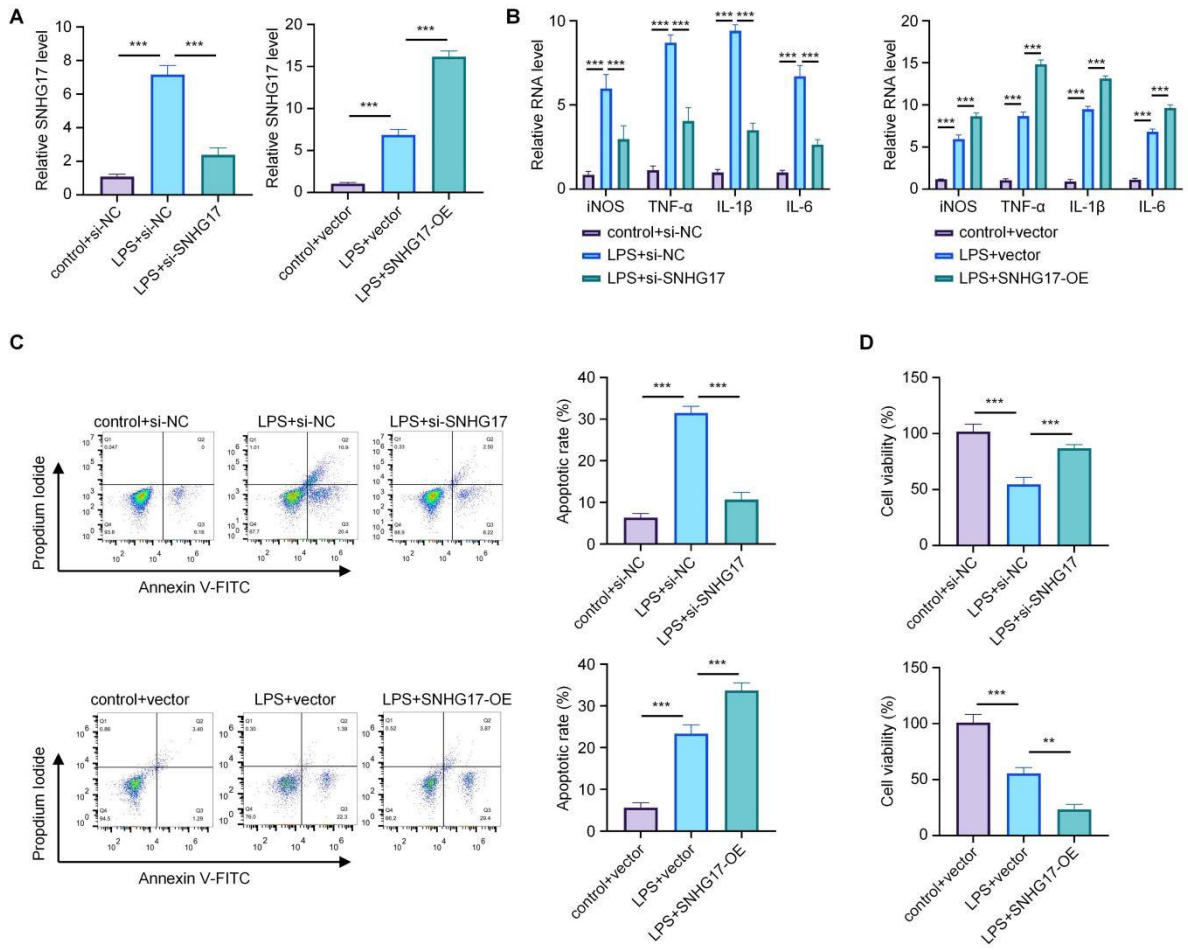

Figure 2. SNHG17 Promotes the Acute Response and Dysfunction in LPS-Induced BV2 Cells

3.3 SNHG17 Regulates LPS-Induced BV2 Cell Inflammation and Apoptosis via miR-381-3p

Bioinformatics analysis showed that snhg17 may play a role as a Cerna of mir-381-3p, thereby exerting its biological effects (Figure 3A). To boost miR-381-3p expression, we transfected BV2 cells with miR-381-3p mimics (Figure 3B). Then, we used a dual-luciferase reporter experiment to see if they interacted. In comparison to the NC group, the experimental group co-transfected with the SNHG17 wild-type plasmid and miR-381-3p mimics displayed around a 70% decrease in fluorescence (Figure 3C). SNHG17 can exercise its biological effects in SCI by acting as a sponge for miR-381-3p. qPCR was used to assess the expression of iNOS, TNF α , IL1 β , and IL6 in cells from each group after miR-381-3p was overexpressed. The results showed that iNOS, TNF α , IL-1 β , and IL-6 levels decreased when miR-381-3p was

overexpressed (Figure 3D). The findings of the CCK8 assay showed that after translation of miR-381-3p, cell viability increased (Figure 3ED). Flow cytometry investigations revealed that overexpression of miR-381-3p reduced the proportion of apoptotic cells (Figure 3F). The aforementioned findings demonstrated that the generation of mir-381-3p could prevent BV2 cell death and the inflammatory response brought on by lipopolysaccharide (LPS).

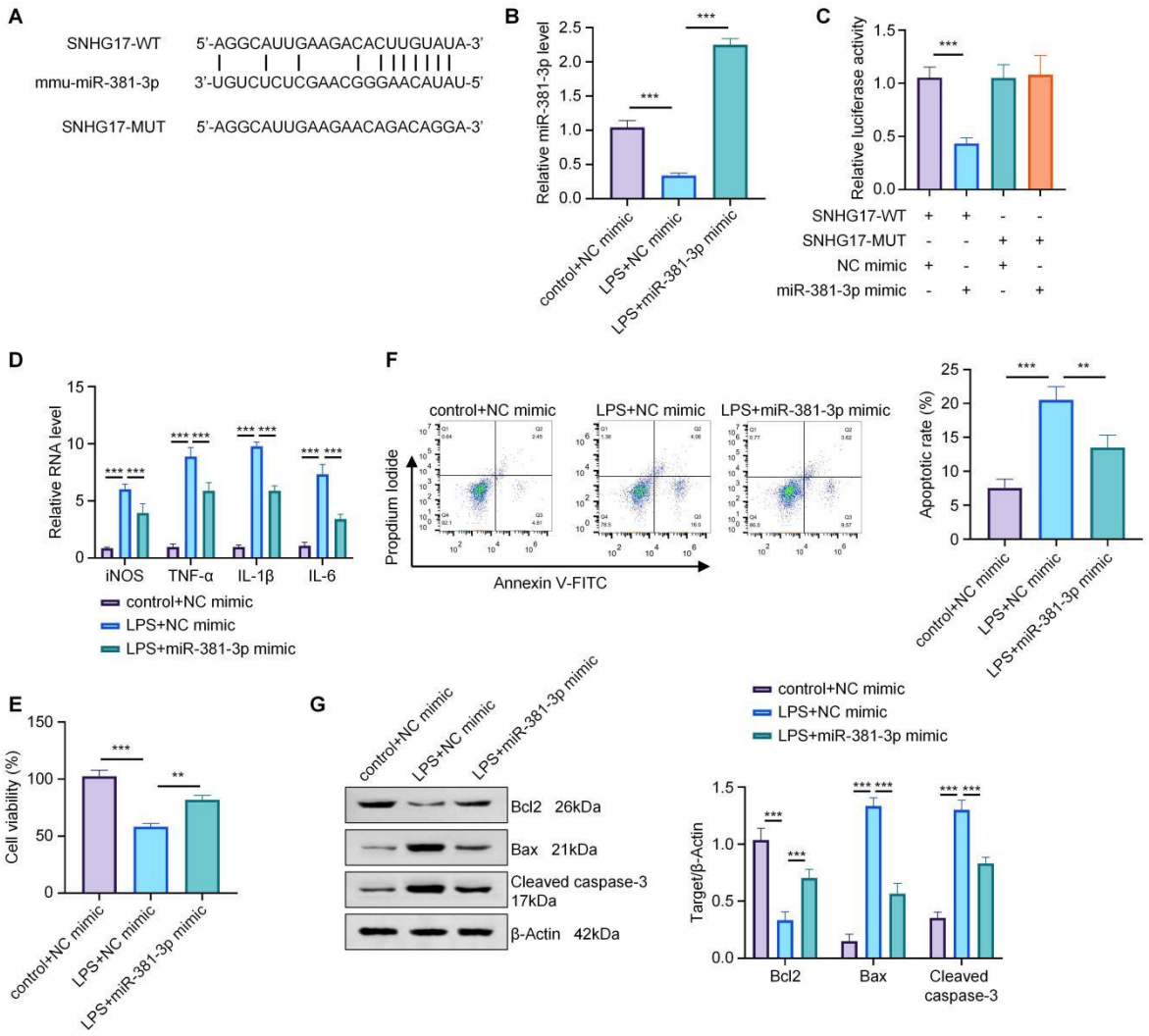

Figure 3. Overexpression of miR-381-3p inhibits LPS-induced apoptosis and inflammation in BV2 cells.

To explore the regulatory effect of snhg17 on mir-381-3p, a functional rescue experiment for SNHG17 was implemented in BV2 cells by utilization of miR-381-3p. RT-qPCR test results displayed that, when making a comparison with the LPS + si-SNHG17 group, In LPS+si-snhg17+mir-381-3p inhibitor group, the concentrations of iNOS, TNF - α, IL-1 β and IL-6

increased, while the LPS+si-SNHG17+miR-381-3p mimic group exhibited reduced levels of these markers relative to the inhibitor group and were the lowest among the four groups (Figure 4A). The CCK8 assay revealed that the cell viability of the lps+si-snhg17+mir-381-3p inhibitor group was lower than that of the lps+si-snhg17 group. As a result, the lps+si-SNHG17+mir-381-3p mimic group's cell viability was greater than that of the inhibitor group; consequently, its viability rebounded to a level comparable to that of the LPS+si-SNHG17 group, as shown in Figure 4B. However, compared to the inhibitor group, the LPS + si-snhg17 + mir-381-3p mimics group had the lowest apoptosis level among the four groups (Figure 4C).Thus, these outcomes lead to the implication that SNHG17 regulates the inflammation and apoptosis which are induced by LPS in BV2 cells via miR-381-3p.

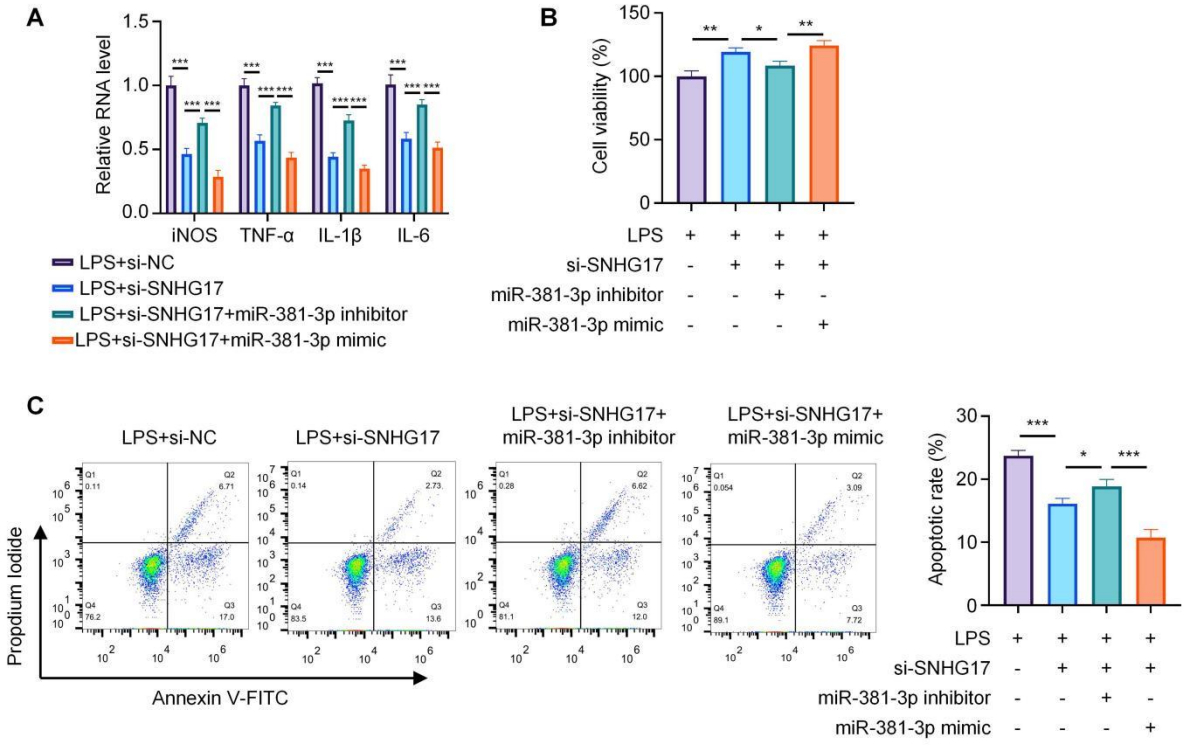

Figure 4. SNHG17 Regulates LPS-Provoked Inflammation and Apoptosis inside BV2 Cells via miR-381-3p

3.4 miR-381-3p Regulates LPS-Induced Inflammation and Injury in BV2 Cells via RAP1B

The ability of long non-coding RNAs (lncRNAs) to behave as miRNA sponges influences the ability of miRNAs to govern the activation of the genes they control. Therefore, this situation will bring about changes to the amounts of target gene expression and further modify the biological functions of tumor cells. The possible target genes of miR-139-5p were predicted in this particular research activity. The 3' untranslated region (UTR) of RAP1B was found to include binding sites for miR-381-3p, as seen in Figure 5A. As illustrated in Figure 5B, a dual-luciferase reporter experiment was employed to confirm the interaction between these two components. The expression of miR-381-3p and RAP1B was individually regulated in BV2 cells in order to examine the regulatory impact of miR-381-3p on RAP1B. RAP1B levels decreased as a result of miR-381-3p overexpression, according to RT-qPCR results (Figure 5C). RT-qPCR was used to assess the expression changes of iNOS, TNF-α, IL-1β, and IL-6 in each group after RAP1B knockdown in BV2 cells (Figure 5D). The results showed that iNOS, TNF-α, IL-1β, and IL-6 levels decreased when RAP1B expression was reduced (Figure 5E). CCK8 examination outcomes displayed that cell viability had rise in the RAP1B knockdown group (Figure 5F). Flow cytometry analysis made known that apoptotic cell proportion had reduction in the RAP1B knockdown group (Figure 5G). Furthermore, the RAP1B knockdown group had lower levels of cleaved Caspase-3 and Bax and higher levels of Bcl-2, according to Western blot results (Figure 5H). Therefore, hence, these results indicate that RAP1B knockdown can inhibit LPS-caused inflammation and apoptosis inside BV2 cells.

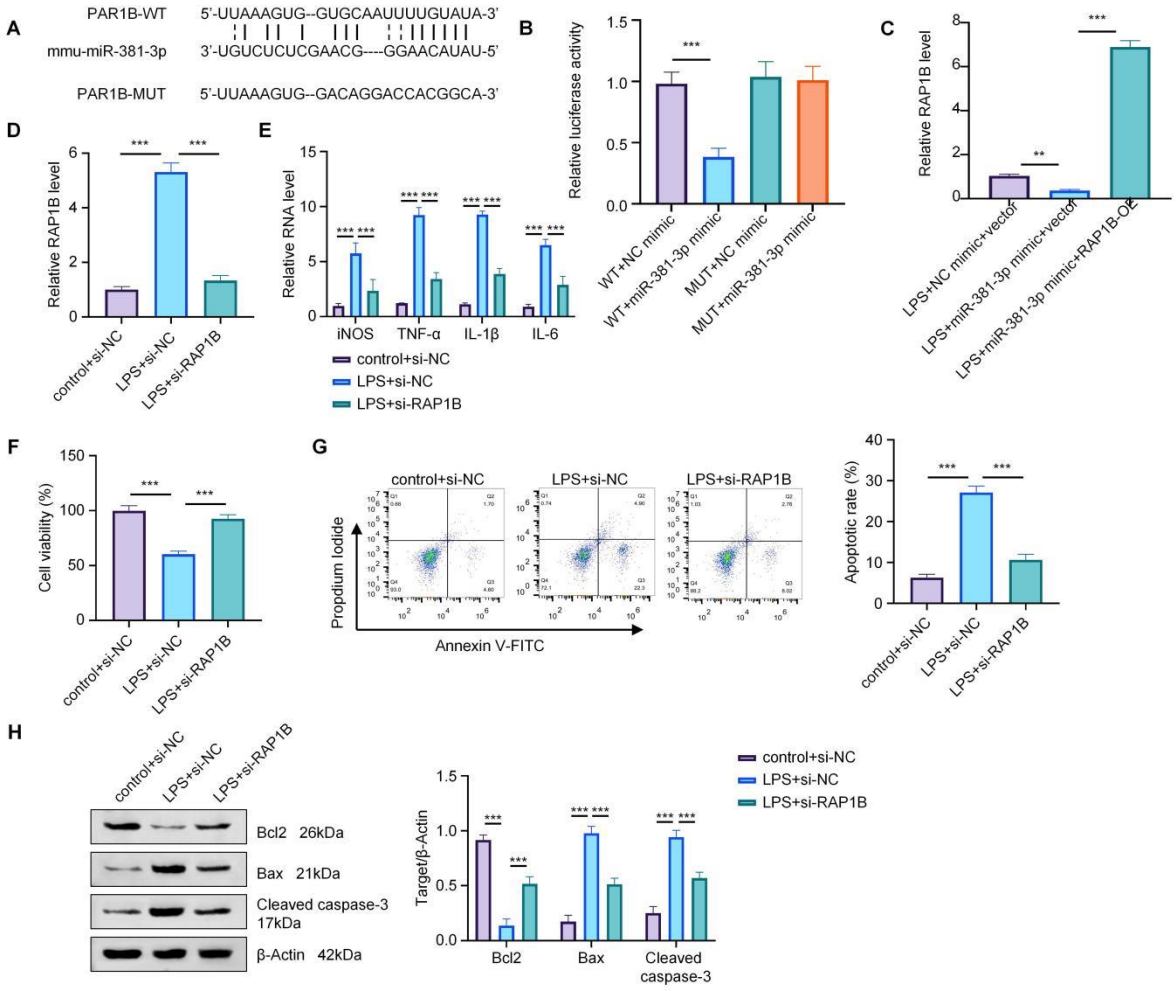

Figure 5. RAP1B Knockdown Action Restrains LPS-Caused Inflammation and Apoptosis Phenomenon in BV2 Cells.

Functional rescue experiments were carried out in BV2 cells to investigate the regulatory effect of miR-381-3p on RAP1B. Based on RT-qPCR results, The LPS + miR-381-3p mimic + vector group had lower levels of iNOS, TNF-α, IL-1β, and IL-6 than the control group. Thus, the LPS + miR-381-3p mimic + RAP1B overexpression group showed higher levels of these markers than the LPS + miR-381-3p mimic + vector group.(Figure 6A). First, the results of the CCK8 assay clearly showed that the LPS + miR-381-3p mimic + vector group had more cell viability than the control group. Consequently, compared to the LPS + miR-381-3p mimic + vector group, cell viability was lower in the LPS + miR-381-3p mimic + RAP1B overexpression group (Figure 6B). Furthermore, the results of the flow cytometry test indicated that the LPS + miR-381-3p mimic + vector group had a lower percentage of dead cells displaying apoptotic

characteristics than the control group. In contrast to the LPS + miR-381-3p mimic + vector group, the RAP1B-OE group had a higher percentage of apoptotic cells. (Figure 6C). Additionally, compared to the control group, the LPS + miR-381-3p mimic + vector group had lower levels of Bax and cleaved Caspase-3 and higher levels of Bcl-2, according to Western blot analysis. However, the LPS + miR-381-3p mimic + RAP1B overexpression group revealed higher levels of Bax and cleaved Caspase-3 and lower levels of Bcl-2 when compared to the LPS + miR-381-3p mimic + vector group. (Figure 6D). In conclusion, miR-381-3p uses RAP1B to control the inflammation and damage brought on by LPS in BV2 cells.

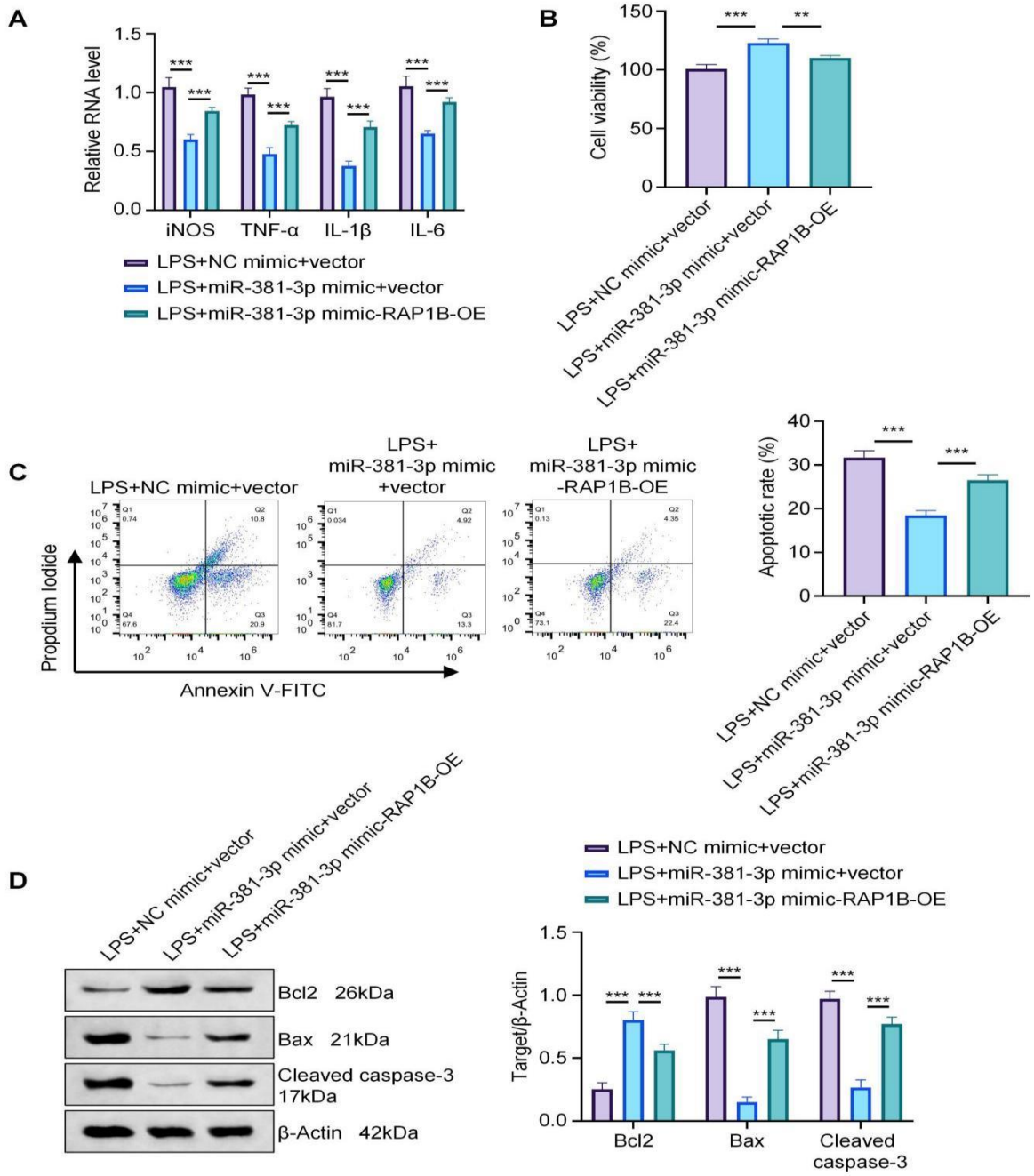

Figure 6. miR-381-3p Modifies LPS-Induced Inflammation and Damage in BV2 Cells via RAP1B

3.5 SNHG17 Improves Spinal Cord Inflammation and Injury in SCI Mice via the miR-381-3p/RAP1B Axis

To make a more deep-going investigation about SNHG17’s function and inner mechanism in mice, adeno-associated viruses were used to change SNHG17’s expression inside mouse spinal cord tissue (Figure 7A). As a result, RT-qPCR analysis revealed increased levels of miR-381-3p in the spinal cord tissue of mice with SNHG17 knockdown.(Fig. 7B). RAP1B levels were lower in the spinal cord tissue of mice in the SNHG17 knockdown group, according to Western blot data (Figure 7C). Hence, this further proved that SNHG17 has regulatory effect on miR-381-3p/RAP1B’s expression. BBB scoring results revealed that BBB score was higher in mice of the SNHG17 knockdown group (Figure 7D). Thus, behavioral experiment data showed that grid-walking test’s error rate was lower in mice of the SNHG17 knockdown group (Figure 7E). Footprint analysis results indicated that the score was higher in mice of the SNHG17 knockdown group (Figure 7F), and thus, these results imply that SNHG17 knockdown improved mice's hindlimb motor function following spinal cord injury (SCI).

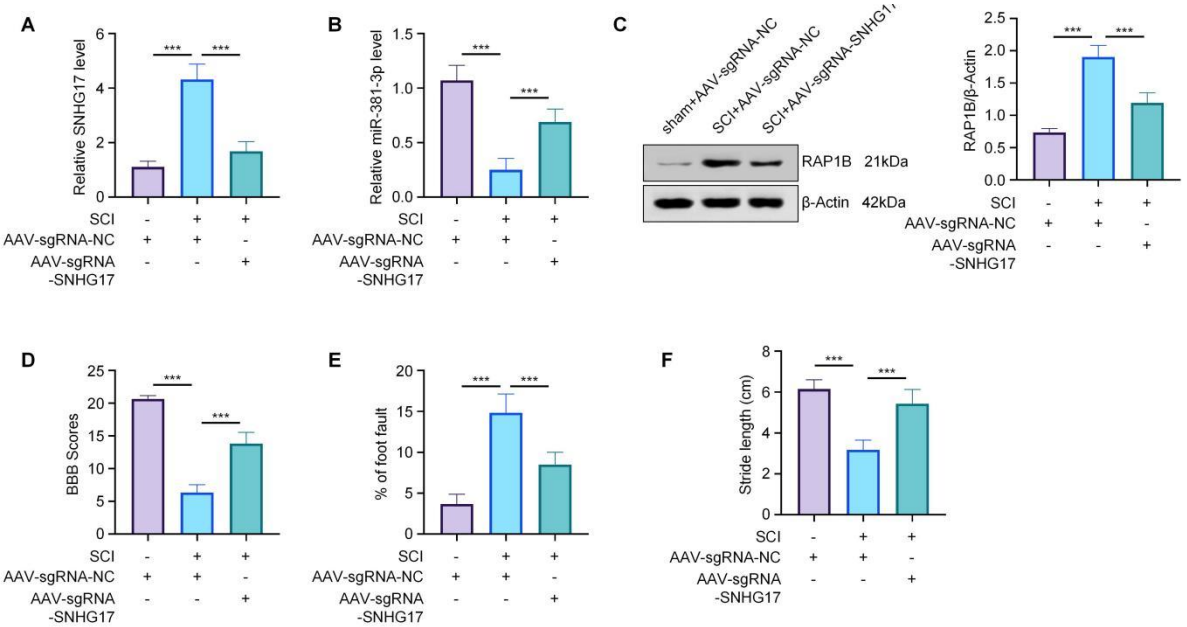

Figure 7. Knockdown of SNHG17 Treatment Improves Hindlimb Motor Function in Mice after SCI

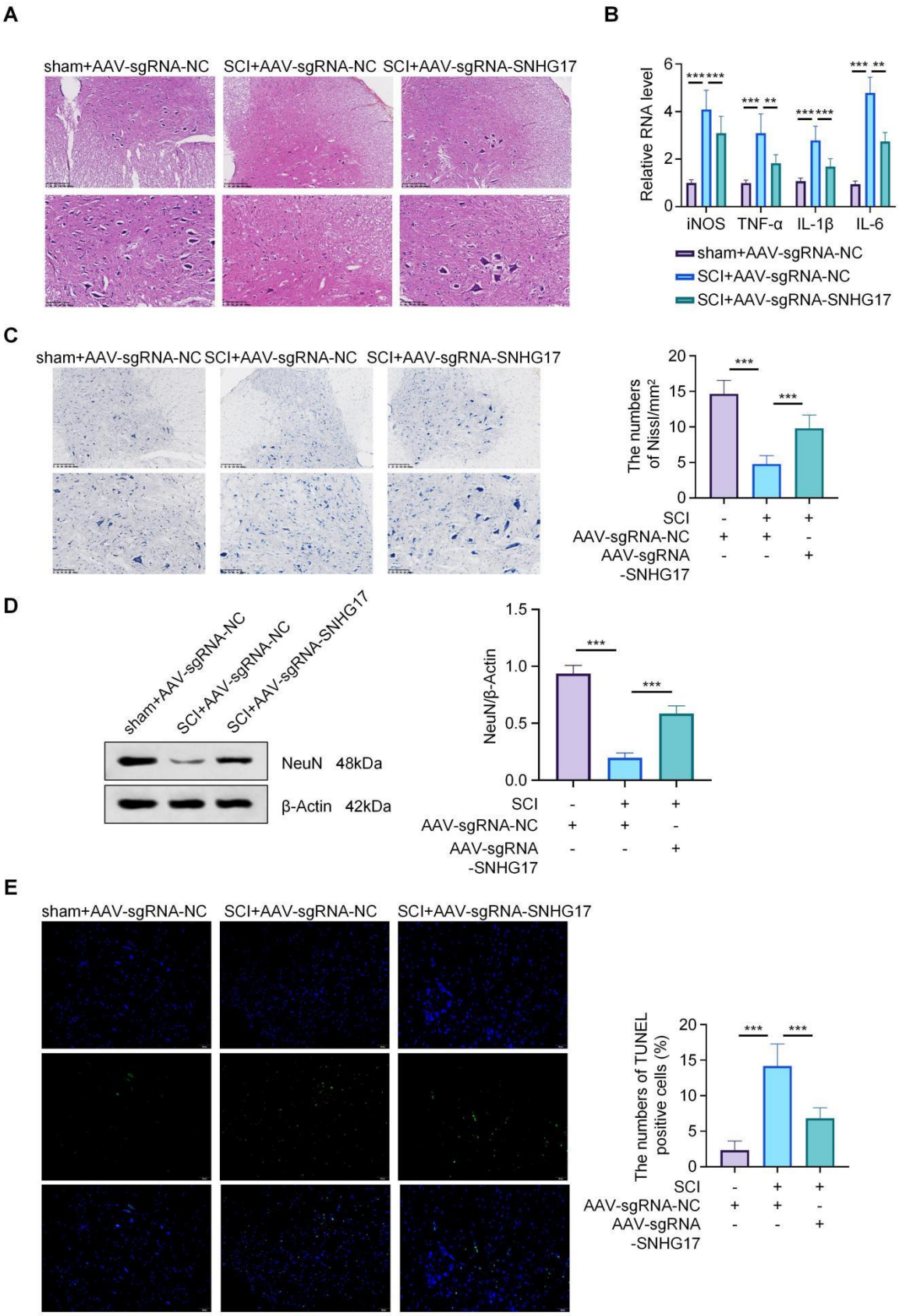
A
sham+AAV-sgRNA-NC
SCI+AAV-sgRNA-NC
SCI+AAV-sgRNA-SNHG17
B
Relative RNA level
iNOS
TNF-α
IL-1β
IL-6
sham+AAV-sgRNA-NC
SCI+AAV-sgRNA-NC
SCI+AAV-sgRNA-SNHG17
C
sham+AAV-sgRNA-NC
SCI+AAV-sgRNA-NC
SCI+AAV-sgRNA-SNHG17
The numbers of Nissl/mm²
SCI
AAV-sgRNA-NC
AAV-sgRNA -SNHG17
D
sham+AAV-sgRNA-NC
SCI+AAV-sgRNA-NC
SCI+AAV-sgRNA-SNHG17
NeuN 48kDa
β-Actin 42kDa
NeuN/β-Actin
SCI
AAV-sgRNA-NC
AAV-sgRNA -SNHG17
E
sham+AAV-sgRNA-NC
SCI+AAV-sgRNA-NC
SCI+AAV-sgRNA-SNHG17
The numbers of TUNEL positive cells (%)
SCI
AAV-sgRNA-NC
AAV-sgRNA -SNHG17

Figure 8. SNHG17 Improves Spinal Cord Inflammation and Injury in SCI Mice via the miR-381-3p/RAP1B Axis

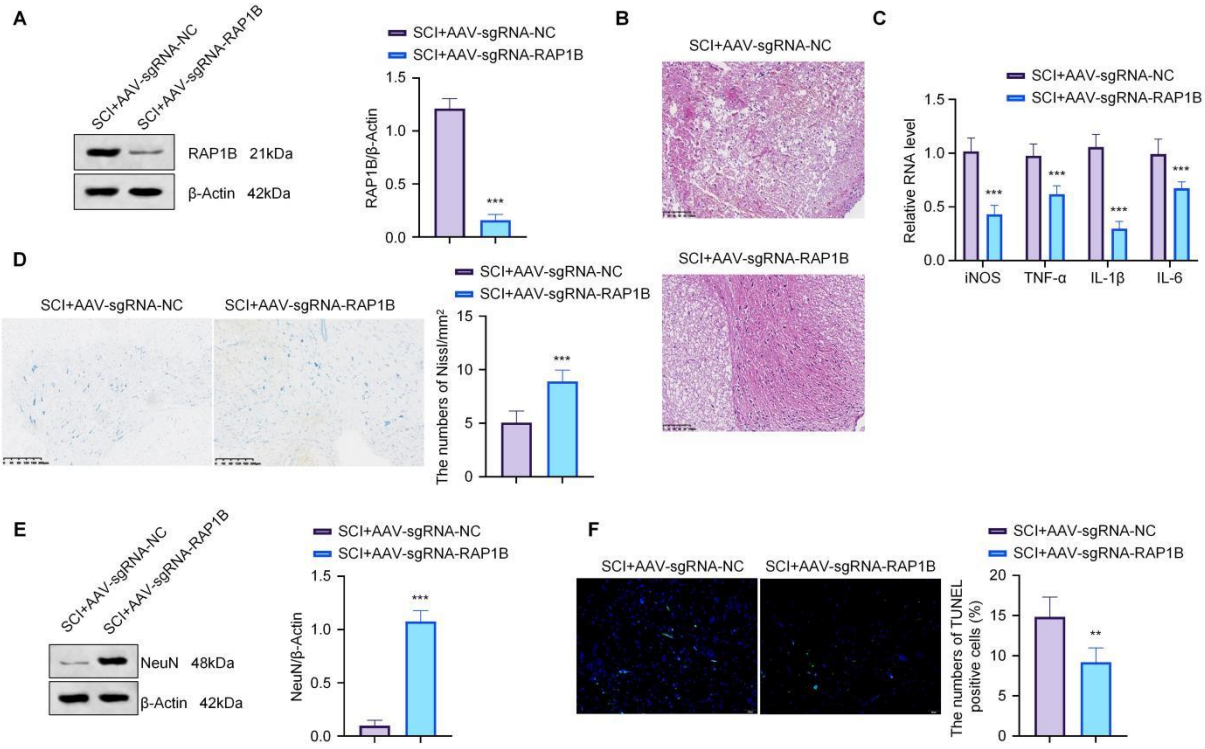

Figure S1. Knockdown of RAP1B Alleviates Inflammation and Pathological Damage in SCI Mice

4 Discussion

Long non-coding RNAs (lncRNAs) are RNA molecules longer than 200 nucleotides that do not encode proteins. However, recent studies have reported that some non-coding RNAs (ncRNAs) may encode micropeptides[19]. Small nucleolar RNA host gene 17 (SNHG17) is a long non-coding RNA that is 1,186 nucleotides in length, belonging to the SNHG family, and is located on human chromosome 20q11.23.Like other members belonging to the SNHG family, SNHG17 has been recorded to hold oncogenic properties. It promotes tumor cell proliferation, invasion, migration, and angiogenesis; at the same time, it inhibits apoptosis. Furthermore, SNHG17 shows different biological functions in other pathological situations, including

pregnancy-related problems, type 2 diabetes, and diabetic nephropathy. Therefore, in this study, we first performed bioinformatics analysis on the mouse spinal cord injury SCI microarray data obtained from the GEO database. The analysis revealed that SNHG17 expression levels were elevated in SCI cases. Hence, to further verify this discovery and research the function of SNHG17, we established an SCI mouse model and an LPS-induced inflammation model by using BV2 cells. Compared with the sham group, we observed a very big rise of SNHG17 expression in spinal cord tissue. Therefore, this result is in line with bioinformatics prediction, hence indicating that SNHG17 may have a function in pathophysiological occurrences after SCI. A same situation was found in LPS-induced BV2 cell inflammation model. Thus, this further suggests SNHG17 may have a possible connection with SCI-related inflammation and cell damage. In order to make clear the specific function of SNHG17, we used siRNA knockdown and overexpression plasmid transfection methods to adjust its function inside BV2 cells.

MicroRNAs are natural-existing non-coding ribonucleic acids. Under various pathological and physiological conditions, their expression has changes, It may be detectable in bodily fluids. Therefore, further detailed research is required regarding the utility of microRNA as a biomarker for spinal cord injury (SCI)[18, 21]. This research takes miR-381-3p as the central object, probing into its function and inner mechanism in SCI. The research indicates that SNHG17 exhibits regulator-like behavior and acts as a sponge for miR-381-3p. Overexpression of miR-381-3p may effectively prevent inflammation and mortality in BV2 cells produced by lipopolysaccharide (LPS) in cellular function tests. This reveals unequivocally the protective effect of miR-381-3p in cell stress responses linked to spinal cord injury (SCI). The process is achieved by regulating intracellular inflammation and the signalling cascades that initiate cell death., it has the capacity to reduce cell damage caused by SCI, thus this could potentially produce a large influence on the pathological progress of SCI. Subsequent research discovered the mechanism that miR-381-3p targets and controls RAP1B. Therefore, we put forward the hypothesis that after SCI occurs, miR-381-3p may protect neurons after SCI by inhibiting the expression of RAP1B, and thus regulate cellular inflammation and apoptosis responses. Hence, this regulatory axis might be an important component within the pathological mechanism of SCI. This compelling demonstrates that miR-381-3p plays a crucial protective role in the cell stress responses associated with spinal cord injury (SCI). Through adjustment of the intracellular inflammation and apoptosis signal paths, it can reduce the cell damage that is caused by SCI. Hence, this may produce a notable influence on the pathological development process of SCI. Later researches have found out the mechanism which miR-381-3p uses to target and control RAP1B. Therefore, we put forward the hypothesis that after SCI occurs, miR-381-3p may

provide protection to neurons post SCI by inhibiting the expression of RAP1B, and thus adjust the cellular inflammation and apoptosis reactions. Therefore, this regulatory axis could be a notable component inside the pathological mechanism of SCI.

Despite the notable research results that have been put forward above, some limitations are still existing. This work focuses on the function of SNHG17 in the initial phases of inflammation and cell death following spinal cord injury (SCI).SNHG17's function in the latter phases of neurogenesis, healing, and functional restoration after SCI has not yet been investigated. The experimental verification work of this study was only conducted on mouse model and BV2 cell line. Although mouse model is widely applied and has representativeness in SCI research, the pathophysiological mechanisms of human SCI are probably more complex because of species differences. Consequently, to encourage the application of these study findings in clinical practice, it is necessary to further confirm the reliability and effectiveness of the study’s results by using human specimens or animal models that are more similar to human physiological states, such as primate models.

Ultimately, our research made the determination that long non-coding ribonucleic acid SNHG17 makes spinal cord injury become more severe via the miR-381-3p/RAP1B axis. Therefore, thus, In rats with injured spinal cords (SCI), silencing SNHG17 can improve motor function and lessen inflammation and damage to the spinal cord.

References:

[1] Khorasanizadeh M, Yousefifard M, Eskian M, et al. Neurological recovery following traumatic spinal cord injury: A systematic review and meta-analysis [J]. J Neurosurg Spine, 2019, 30(5): 683-99.

[2] Ohnmar H, Das S, Naicker A S. An interesting case of Autonomic Dysreflexia [J]. Clin Ter, 2009, 160(5): 371-3.

[3] Oyinbo C A. Secondary injury mechanisms in traumatic spinal cord injury: A nugget of this multiply cascade [J]. Acta Neurobiol Exp, 2011, 71(2): 281-99.

[4] Rodríguez-Barrera R, Ibarra A, Rivas-González M, et al. Neurogenesis after spinal cord injury: State of the art [J]. Cells, 2021, 10(6).

[5] Hejrati N, Fehlings M G. A review of emerging neuroprotective and neuroregenerative therapies in traumatic spinal cord injury [J]. Curr Opin Pharmacol, 2021, 60: 331-40.

[6] Warner F M, Cragg J J, Jutzeler C R, et al. Early Administration of Gabapentinoids Improves Motor Recovery after Human Spinal Cord Injury [J]. Cell Rep, 2017, 18(7): 1614-8.

[7] Zhou L Y, Tian Z R, Yao M, et al. Riluzole promotes neurological function recovery and inhibits damage extension in rats following spinal cord injury: a meta-analysis and systematic review [J]. J Neurochem, 2019, 150(1): 6-27.

[8] Gao S, Zhang Z M, Shen Z L, et al. Atorvastatin activates autophagy and promotes neurological function recovery after spinal cord injury [J]. Neural Regen Res, 2016, 11(6): 977-82.

[9] Kwon B K, Okon E, Hillyer J, et al. A systematic review of non-invasive pharmacologic neuroprotective treatments for acute spinal cord injury [J]. J Neurotrauma, 2011, 28(8): 1545-88.
[10] Liang Guohui, Zhou Yingjie, Xie Yan, et al. The regulatory pathway of neurotransmitters regulation existing in rats with spinal cord injury [J]. Chinese Journal of Orthopedics of Traditional Chinese Medicine, 2023,31 (07): 6-11.
[11] Many Fang, Zhang Yanjun, Guo Tiefeng, et al. The role of long non-coding RNA in secondary spinal cord injury and the research progress of TCM intervention [J]. Western Traditional Chinese Medicine, 2025,38 (01): 99-105.
[12] Tan Xiuwei, Wu Yanli, Li Fengxin, et al. Regulation of lncRNA HOTAIR / NF- κ B to promote motor function after spinal cord injury [J]. Journal of Guangxi Medical University, 2024,41 (05): 681-7.
[13] Strickland E R, Hook M A, Balaraman S, et al. MicroRNA dysregulation following spinal cord contusion: Implications for neural plasticity and repair [J]. Neuroscience, 2011, 186: 146-60.
[14] Yunta M, Nieto-Díaz M, Esteban F J, et al. MicroRNA dysregulation in the spinal cord following traumatic injury [J]. PLoS ONE, 2012, 7(4).
[15] Bhalala O G, Srikanth M, Kessler J A. The emerging roles of microRNAs in CNS injuries [J]. Nat Rev Neurol, 2013, 9(6): 328-39.
[16] Hu J R, Lv G H, Yin B L. Altered MicroRNA expression in the Ischemic-Reperfusion spinal cord with atorvastatin therapy [J]. J Pharmacol Sci, 2013, 121(4): 343-6.
[17] Shi Z, Zhou H, Lu L, et al. The roles of microRNAs in spinal cord injury [J]. Int J Neurosci, 2017, 127(12): 1104-15.
[18] Liu Tao, Zhi Zhongzheng, Wang Yingjie, et al. LncRNA GAS5 studied the mechanism of regulating nerve cell apoptosis after spinal cord injury through miR-21 [J]. Orthopaedics, 2024,15 (02): 145-54.
[19] Wu P, Mo Y, Peng M, et al. Emerging role of tumor-related functional peptides encoded by lncRNA and circRNA [J]. Mol Cancer, 2020, 19(1).
[20] Ergin K, Çetinkaya R. Regulation of MicroRNAs [Z]. Methods in Molecular Biology. Humana Press Inc. 2022: 1-32.10.1007/978-1-0716-1170-8_1
[21] Yang Qinglin, Wang Yukun, Qin Qingqing, et al. Role of non-coding RNA in spinal cord injury [J]. Chinese Journal of Cell Biology, 2023,45 (06): 974-81.